

UNCLASSIFIED

AD 407 317

DEFENSE DOCUMENTATION CENTER

FOR

SCIENTIFIC AND TECHNICAL INFORMATION

CAMERON STATION, ALEXANDRIA, VIRGINIA



UNCLASSIFIED

NOTICE: When government or other drawings, specifications or other data are used for any purpose other than in connection with a definitely related government procurement operation, the U. S. Government thereby incurs no responsibility, nor any obligation whatsoever; and the fact that the Government may have formulated, furnished, or in any way supplied the said drawings, specifications, or other data is not to be regarded by implication or otherwise as in any manner licensing the holder or any other person or corporation, or conveying any rights or permission to manufacture, use or sell any patented invention that may in any way be related thereto.

CATALOGED BY DDC

AS AD No. 407317

407 317

63.4

ARTHUR D. LITTLE, INC.

INTERIM ENGINEERING REPORT NO. 5

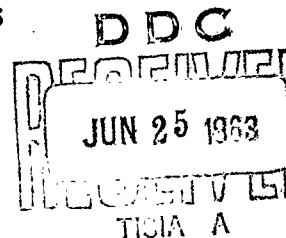
SUPERCONDUCTIVE EFFECTS IN THIN FILMS

S. SHAPIRO

REPORT PERIOD 15 JANUARY - 15 APRIL 1963

CONTRACT NO. AF33(657)-7915

BPSN: 36799-760E-446002



The applied research reported in this document has been made possible through support and sponsorship extended by the Aeronautical Systems Division, Air Force Systems Command, United States Air Force, under Contract No. AF33(657)-7915. It is published for technical information only and does not necessarily represent recommendations or conclusions of the sponsoring agency.

Arthur D. Little, Inc.

C-64380

Interim Engineering Report Nr. 5

"Superconductive Effects in Thin Films"

S. Shapiro

15 May 1963

Report Period: 15 January 1963 - 15 April 1963

Contract Nr. AF33(657)-7915

BPSN 36799-760E-446002

"The applied research reported in this document has been made possible through support and sponsorship extended by the Aeronautical Systems Division, Air Force Systems Command, United States Air Force, under Contract Nr. AF33(657)-7915. It is published for technical information only and does not necessarily represent recommendations or conclusions of the sponsoring agency."

ABSTRACT

The present report covers the fifth three months of effort in an applied research program in which determining the feasibility of performing electronic functions by making use of the phenomenon of electron tunneling between superconductors has been the chief object.

Improvements were made in the measurement of microwave cavity Q. A cw local oscillator beating against the fm signal klystron generates a band of beat frequencies. A tunable radio receiver selects the desired narrow band. After shaping by an RC circuit, this band is used to trigger a pulse generator resulting in a pair of very sharp markers separated by a controllable and accurately measurable amount in frequency. Thus the bandwidth of the cavity characteristic can be accurately determined leading to a much improved Q measurement.

Efforts were made to prepare low resistance tunneling crossings with thin Al and Sn films. Stability with time of such crossings was poor. By using gaseous anodization and thick Sn films, low resistance crossings with slow enough growth curves for experimentation were formed.

Despite the use of thin Al films in low resistance crossings, or the use of poor RC crossings, no quantum effects were observed in the presence of microwave power. It was noted that magnetic flux was sometimes trapped in the films forming the sample. This resulted in substantial rounding of the sharp corner in the I-V characteristic and care was taken to avoid the effect. The square wave response of a sample operated as a microwave detector was examined up to the limit of the oscilloscope used, less than 1 megacycle. The tunneltron response was found not limiting.

Zero-voltage currents associated with the tunneling of electron pairs have been observed in all low resistance samples. An ac technique was used which permitted a demonstration that these currents were not due to superconducting short circuits. The technique also illustrated that the zero-voltage currents decayed to the familiar single-particle tunneling characteristic via a negative resistance. Rf oscillations in appropriately designed oscillator circuits have been observed associated with this region.

Excess ac at zero-voltage was also observed. Sometimes with a random behavior from cycle to cycle. The temperature dependence of the pair-tunneling currents was demonstrated.

Apparatus has been designed and constructed for extending the microwave measurements to 4 mm. and 2 mm. wavelength. A shorted waveguide is used rather than a resonant cavity. The sample is formed on a 2-mil quartz substrate and has a crossing area of 1 square mil. It sits in the center of the waveguide exposed to microwave electric field.

Table of Contents

	<u>Page</u>
I. Introduction	1
II. X-Band Microwave Experiments	1
A. Measurement of Cavity Q	1
B. Comments on Sample Preparation	4
C. Miscellaneous Observations	8
D. Zero-Voltage Currents in Superconducting Tunneling	9
III. Millimeter Wave Experiments	16
IV. Conclusions	20
V. Recommendations	21
References	22

I. Introduction

The major purpose of this report is to discuss a few topics which have not heretofore been treated in these reports but to which some effort has been directed. Among these topics are the technique and apparatus developed for reasonably accurate measurement of the Q of the microwave cavity; some comments and experiments on sample preparation; and the design details relative to the experimental system for the planned millimeter wave experiments. In addition, the X-band experiments are brought up to date and new observations on tunneling in thin dielectric specimens are reported.

II. X-Band Microwave Experiments

A. Measurement of Cavity Q

As discussed in previous reports, knowledge of the unloaded Q , Q_u , of the microwave cavity is essential in converting power readings to values of field intensity and eventually to rf voltage. Measurement of the cavity resonant frequency, f_c , and full bandwidth between half-power points, Δf_c , determine the loaded Q , Q_L , through the relation

$$Q_L = f_c / \Delta f_c. \quad (1)$$

The unloaded Q is determined from Q_L and the cavity coupling coefficient, η , from

$$Q_u = Q_L (1 + \eta). \quad (2)$$

In turn, η is obtained either from measurement of the VSWR, r , or the power reflection coefficient, Γ^2 , through the relations

$$\eta = 1/r \text{ (undercoupled cavity)} \quad (3)$$

or,

$$\eta = \frac{1 - \Gamma}{1 + \Gamma}. \quad (4)$$

Previous to the development of the apparatus described below, the quantity, Δf_c , was determinable only with indifferent accuracy. All other quantities were speedily measurable to a per cent or so. The present apparatus permits Δf_c to be measured also to within a few per cent by providing sharp frequency markers whose separation may be readily varied and accurately determined.

The technique is to beat a local oscillator, operated cw at f_c , against an fm signal derived from the signal klystron and centered about f_c . This gives rise to a band of beat frequencies, a narrow portion of which is selected by a tunable rf receiver. The two frequency pips derived in this manner are used to trigger a pulse generator and thus are narrowed further. In this manner the height, width, and frequency separation of the pips are controlled to provide the desired resolution in measuring Δf_c .

To accomplish this measurement the microwave circuit has been modified according to the block diagram of Figure 1. A 10 db directional coupler diverts some of the output of the frequency modulated signal klystron to one arm of a magic tee. Another arm of the tee is fed from a local oscillator klystron operated cw. The output of the tee contains the two superimposed waves which are mixed in a detector (No. 2 in the figure).

The output of the mixer detector contains a band of beat frequencies from dc to the greatest difference in frequency between the fm and cw signals. The tunable radio receiver selects the desired portion of that band. The receiver output, displayed as a function of

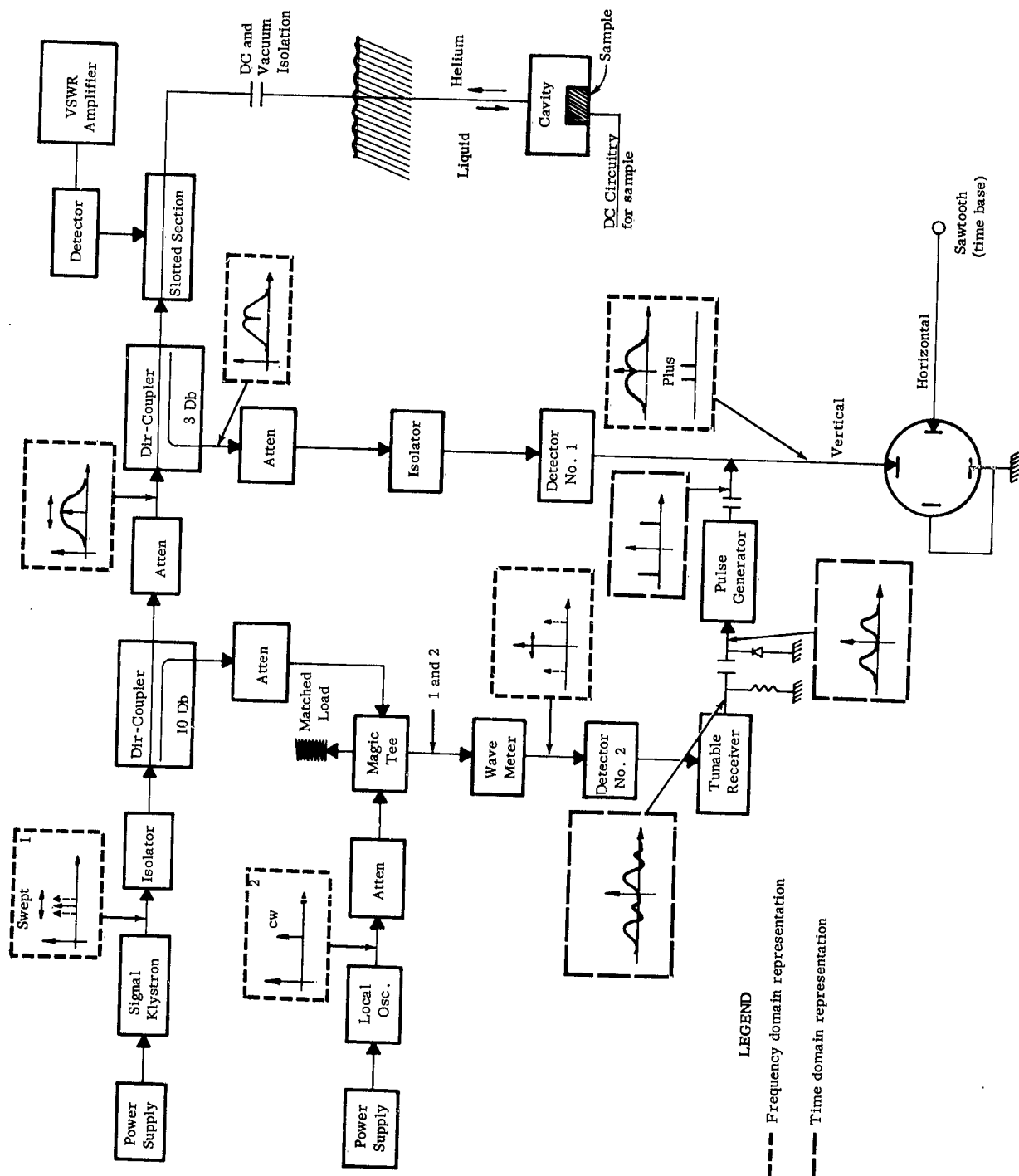


FIGURE 1
MICROWAVE SCHEMATIC INDICATING OPERATION OF C-11

time, shows two pass bands, one corresponding to the time at which $f_{fm} + f_{cw}$ equals the tuned frequency and the other to the time at which this frequency is equal to $f_{fm} - f_{cw}$. The amplitude of the pass bands, which is highest at the tuned frequency, is controlled by varying the gain of the receiver. The frequency spread is fixed by the receiver response.

After some pulse shaping in an RC network, the receiver output pulses are used to trigger a pulse generator. By careful control of the input amplitude and the pulse width, the output pulses may be made very narrow indeed. Their frequency separation is equal to twice the frequency to which the radio receiver is tuned.

By matching the position and separation of the spikes to the half-power points on the cavity characteristic, Δf_c is accurately determined. Figure 2 shows a portion of a typical characteristic and typical frequency marker pips. The base line, corresponding to the zero level of reflected power, is also shown. The frequency separation between the indicated markers is 1.8 Mcps and is less than Δf_c . The loaded Q of the cavity pictured is 4,300 and the unloaded Q is 5,100.

B. Comments on Sample Preparation

In order to investigate the difference in microwave detection results between this work and that of the Bell Telephone Laboratories workers discussed in the Fourth Interim Engineering Report, some effort was devoted toward the preparation of low resistance tunneling crossings employing thin metal films. Effort was concentrated on forming Al-Al₂O₃-Sn tunneling samples. After the failure of the initial attempts, the evaporator was equipped with the necessary electrical feedthroughs, etc., so that the resistance of the metal films and of the tunneling crossings could be examined within the vacuum system.

Electrically continuous Al films of 200Å thickness were readily deposited on conventional glass microscope slides. The slides were cleaned by washing in strong detergent followed by vapor degreasing and,

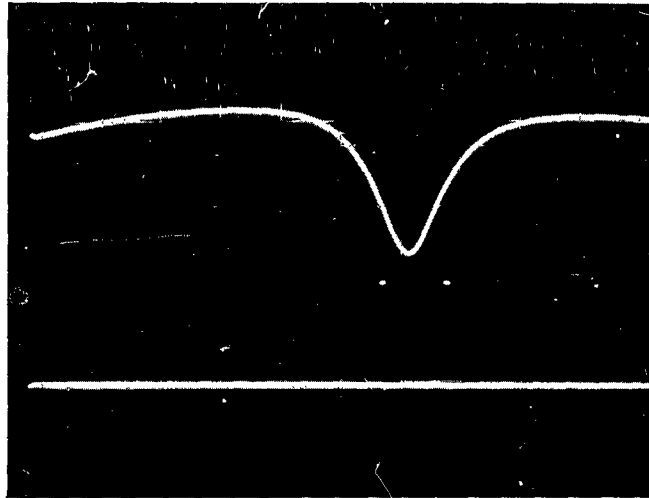


FIGURE 2 FREQUENCY MARKERS SHOWN RELATIVE TO CAVITY CHARACTERISTIC AND BASELINE

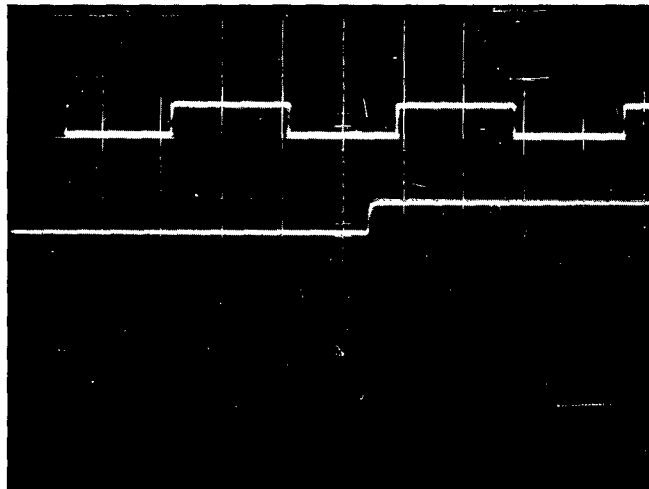


FIGURE 3 TUNNELTRON DETECTED SQUARE-WAVE SIGNAL. VERTICAL SCALE, 1 mV/CM. TIME BASE: UPPER TRACE, 0.1 M SEC./CM.; LOWER TRACE, 20 μ SEC./CM.

in the vacuum system, an ion bombardment treatment. In order to achieve low ohms per square, it proved desirable to deposit initially a non-conducting gold film on the glass slide. The gold flash provides, apparently, the required nucleation sites for the subsequently deposited Al film. With the use of the gold flash, the 200Å Al films (approximately 0.260 inch long by 0.0045 inch wide) had resistance values between 1,000 and 2,000 ohms. Without the gold flash, similar films had resistances an order of magnitude higher.

Electrically continuous films were formed at about 500Å of tin, and films of 1000Å thickness or higher exhibited relatively low ohms per square. However, the structure of such films was extremely porous. The porous structure, which has the appearance of worm holes, persisted even to thicknesses as great as 3000Å, as was made clear from electron micrographs. Only slight differences in the film structure were achieved by varying the deposition rate onto the uncooled substrate.

With this information about the metal films, it was decided to employ 200Å Al films but thick Sn films in forming the tunneling crossings. Low crossing resistance was desired but proved impossible to obtain at first. In fact, when tin films 1500Å thick were deposited across the Al film without any attempt made to grow oxide on the Al first, the crossings were found, generally, to have a small resistance on the order of a few ohms. As soon as air was admitted to the vacuum system, the crossing resistance began to climb reaching values of about 100 ohms in 3 to 4 minutes and attaining about 1000 ohms after 10 minutes. The use of 3000Å tin films slowed the rate of growth. With crossings formed as above from two Al films, the resistance was invariably zero and remained so indefinitely after exposure to air.

In an attempt to gain some understanding of these effects a brief series of experiments was performed. All samples were formed with 200Å Al films deposited after a gold flash as described above. Two tin thicknesses were used, 1500Å and 3000Å. Two rates of tin deposition

were employed; normal, corresponding to about 15\AA per second, and fast, which was about 45\AA per second. Finally, one set of runs was taken without any oxidation treatment of the Al and another set where the Al was dry anodized by a 15-second exposure to a gaseous discharge in an atmosphere of dry oxygen at a pressure of 100 microns of Hg.

Combinations of the six variables resulted in eight sample preparations. No significant structural variations were revealed by electron microscope examination. For each of the samples, the tunneling resistance was monitored as the system was brought to atmospheric pressure and for 10 minutes thereafter.

As long as the system was maintained under vacuum, no change occurred in the resistance. This implies that the substrate cleaning was adequate. It required about 4 minutes to bring the system up to atmospheric pressure. If this was done with air, the resistance changed markedly during this period and afterward. If this was done with dry oxygen, only small changes in tunneling resistance resulted, if any. This behavior indicates that water vapor in the air was primarily responsible for changing resistance with time.

The rate of growth was very slightly less for the samples made with a fast tin evaporation compared to those with normal evaporation. The 3000\AA tin films showed rather less rate of growth than the 1500\AA film. The major effect was noted in the difference between the anodized and unanodized samples. Much slower rates of growth were observed in the anodized samples, even though the tunneling resistances were of the same order as in the nonanodized case.

Attempts to provide encapsulation before exposing the samples to air and thus achieve greater stability were not successful. Arsenic trisulfide glass, SiO_2 , and CdTe films were all tried and were found either to contaminate the vacuum system or to react with the metal films.

For the experiments to be discussed later, the plasma anodization step was employed. The samples were mounted in the apparatus and cooled to liquid nitrogen temperature as quickly as possible to preserve the low resistance value. When maintained at low temperatures, a procedure followed in all cases, the tunneling resistance was stable.

C. Miscellaneous Observations

Some discussion was given in the Fourth Interim Engineering Report of possible explanations for the lack of quantum effects in these microwave experiments. Two such possibilities have now been investigated in the course of continued experiments on superconducting tunneling samples as microwave detectors.

In an attempt to reduce the efficiency of classical detection so as to bring out any quantum effects which may not otherwise be observed, a large area (1.3 mm^2) high resistance (3200Ω) tunneling sample was fabricated and tested. The $\text{Al-Al}_2\text{O}_3\text{-Sn}$ specimen was, as expected, a relatively poor detector; however, as before, no quantum effects were observed. The metal films used were each about 1000\AA thick.

Next, the possibility was explored that substantial microwave field penetration of the superconducting films was required for the observation of the quantum effects. Samples were prepared, as described in the preceding section, in which 200\AA thick Al films and 2000\AA Sn films were used. Consistent with all previous runs, no quantum effects were observed in the detection process. This was true even when data were taken carefully as a function of temperature from the Al transition down to about 0.8° K . Over this range the Al energy gap was observed to vary from a value less than the photon energy, $h\nu$, to a value more than eight times this energy. At the operating frequency of 9300 KMcps , $h\nu$ corresponds to a voltage of about $38\mu\text{V}$. The sensitivity of the oscilloscope presentation of the I-V curves was such that quantum effects would have been observed easily, had they been present. Similar negative

results were obtained for runs in which the sample was exposed to predominantly rf E-field as for those in which it was exposed to predominantly rf H-field.

In the course of these experiments, it was noticed that magnetic flux was sometimes trapped in the superconducting films forming the tunneling sample. The trapped flux had the effect of rounding off appreciably the otherwise sharp corner in the I-V characteristic at the upper end of the negative resistance region. As might be expected, detector performance suffered severely in the presence of the trapped flux. It was possible to permit all or most of it to leak away by quenching the metal films momentarily. Both the Al and Sn films had to be quenched to clear the flux although the major effect was achieved by the quenching of the Al. The problem can be alleviated by suitable care in cooling and working with the samples.

Finally, it proved possible to demonstrate to a limited extent the speed of response of the superconducting tunneling system. The RC time constant of the samples was calculated to be of the order of 5 nanoseconds, using for R the low temperature normal resistance of less than 15 ohms. Figure 3 shows, in the upper trace, the wave form of the signal detected by the tunneling sample. The upper edge corresponds to power off. The time scale is 10^{-4} seconds per large division. The lower trace shows on an expanded scale, the trailing edge of the square wave. Clearly the response of the tunneling device is better than a microsecond. The observation of the response was limited by the frequency response of the oscilloscope used (less than 1 Mcps).

D. Zero-Voltage Currents in Superconducting Tunneling

The first successful calculation of tunneling between superconductors on a microscopic basis was made by Cohen, Falicov, and Phillips¹. They succeeded in devising a rigorous quantum mechanical formulation of the problem in which an interaction Hamiltonian transferring electrons from one side of the dielectric barrier to the other plays an important

role. This Hamiltonian is employed within the operator representation appropriate to the microscopic theory of superconductivity of Bardeen, Cooper, and Schrieffer (BCS)². They worked out their theory for the case of tunneling between a normal and a superconducting metal and derived the experimentally proven result that the derivative in voltage of the tunneling current was proportional to the superconducting density of states.

Josephson³ worked out the case of tunneling between two superconducting metals and found that the theory predicted contributions to the tunneling current in addition to those attributable to single electron tunneling. The additional currents behave as if there were a direct tunneling of electron pairs between the Fermi surfaces of the two metals.

The pair tunneling currents should manifest themselves in several ways. For present purposes only one way need be considered. This prediction is that direct current can be passed through the tunneling sample without any voltage being developed across the sample. Thus the tunneling sample acts as a superconductor to the passage of dc of some small amplitude. These direct currents are referred to as zero-voltage currents in superconducting tunneling. Anderson and Rowell⁴ have reported the probable observation of these zero-voltage direct currents.

In the course of our experiments over the past few months, we have had occasion, as described in previous sections, to fabricate many low resistance Al-Al₂O₃-Sn tunneling crossings (5-20 Ω with a crossing area of 1.5×10^{-4} cm²). Every one of these samples tested has exhibited the zero-voltage currents predicted by Josephson. Anderson and Rowell employed a dc technique to observe the zero-voltage currents; we employed our usual ac technique, with various sweep frequencies, and we could also pass dc through the specimens as desired.

Using an ac display, Figure 4a shows for a typical sample the zero-voltage current predicted by Josephson. During each half cycle of the sweep, current flows through the sample without developing any voltage across it until, at a current which depends upon temperature, crossing resistance, and circuit load line, switching to the familiar single-particle tunneling characteristic occurs along the circuit load line. The switching characteristic is stable and reproducible, and is followed both when the current is increasing and when it is decreasing. It is indicative of a negative resistance.

Other investigators⁵ in this laboratory have observed rf oscillations associated with this region. The samples, placed in appropriately designed oscillator circuits, produced rf at the circuit resonant frequency of about 100 Mcps. The rf oscillations appear to confirm that the Josephson current region decays toward the single-particle tunneling characteristic by means of a negative resistance, despite the fact that we have not been able to trace out any appreciable portion of the negative resistance.

The characteristic as shown in Figure 4a can be traced out with dc and follows exactly the course of the ac display. On occasion, however, much more ac can be carried at zero voltage than dc. This is shown in Figure 4b for the same sample as in Figure 4a. The dc that can be carried is indicated by the switching region clearly visible near the origin. (The change of circuit load line between Figures 4a, 1,000 Ω , and 4b, 100 Ω , accounts for the fact that the dc region in Figure 4b is greater in magnitude than in 4a.) The ac that can be carried before voltage is developed across the sample is about fifteen times as great as the dc. The same trace is obtained for all sweep frequencies employed (8 to 800 cps). This excess ac is affected by electrical transients. Such transients can cause the excess ac to disappear and to reappear but has no effect on the rest of the characteristic. Frequently, in contrast to the figure, the excess current is noisy in character, i.e.,



FIGURE 4a PORTION OF I-V CHARACTERISTIC NEAR ORIGIN SHOWING ZERO-VOLTAGE CURRENT AND NEGATIVE RESISTANCE. SCALES: (V) $58.8 \mu\text{V}/\text{CM.}$, (H) $130 \text{ nA}/\text{CM.}$

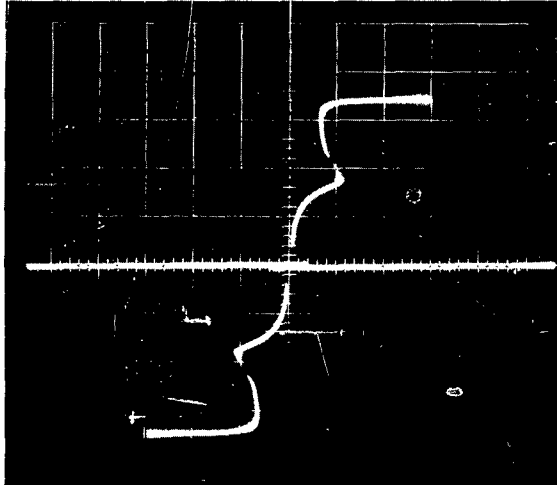


FIGURE 4b I-V CURVE FOR SAME SAMPLE AS ABOVE SHOWING FAMILIAR SINGLE-PARTICLE CHARACTERISTIC AND DC AND AC JOSEPHSON CURRENTS. SCALES: (V) $0.235 \text{ mV}/\text{CM.}$, (H) $2.6 \mu\text{A}/\text{CM.}$

the amplitude of ac carried before switching takes place varies randomly from cycle to cycle. The excess ac appears only at temperatures well below that at which the zero-voltage current is first observed, and is quenched by lower dc magnetic fields and microwave fields than affect noticeably the stable zero-voltage current.

The zero-voltage currents occur only when both metals forming the tunneling sample are superconducting. Thus they should first be observed at the lower critical temperature and should increase in amplitude as the temperature falls and the superconducting energy gap increases. The temperature dependence of the zero-voltage currents has been calculated explicitly by Ambegaokar and Baratoff⁶. Their relation for the supercurrent, J_s , is

$$J_s = R_n^{-1} \epsilon_1(T) K ([1 - \epsilon_1^2(T)/\epsilon_2^2(T)]^{1/2}). \quad (5)$$

In Eq. (5), R_n is the resistance of the tunneling crossing when both metals are normal; $2\epsilon_1(T)$ and $2\epsilon_2(T)$ are the temperature dependent energy gaps for the superconductors ($\epsilon_1 < \epsilon_2$); and K denotes the complete elliptic integral of the first kind.

We have observed the zero-voltage currents as a function of temperature as shown in Figure 5a. The top trace was taken just below the Al transition temperature and the bottom trace was taken about 0.2° K down in temperature. The growth of the current amplitude and the development of the negative resistance described above are clearly shown. Only semi-quantitative data have been obtained; however, the current increases as the temperature falls roughly as predicted by Ambegaokar and Baratoff.

Anderson and Rowell used four criteria to distinguish the pair-tunneling currents from superconducting shorts through the thin insulator. Their criteria have been obeyed by our samples and, in addition, the ac technique has permitted a fifth criterion to be demonstrated.

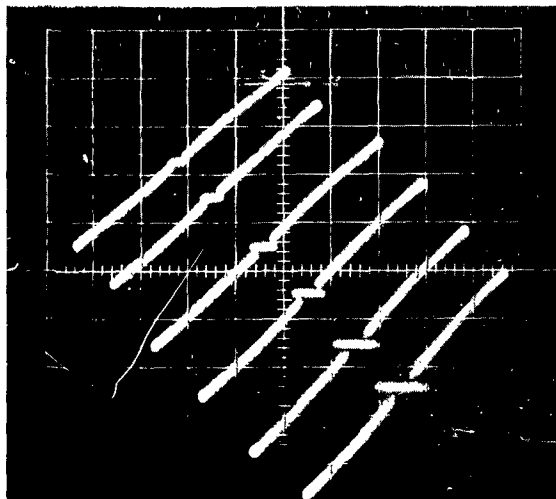


FIGURE 5a SEQUENCE SHOWING TEMPERATURE DEPENDENCE OF JOSEPHSON CURRENT. SCALES: (V) $58.8 \mu\text{V}/\text{CM.}$, (H) $667 \text{ nA}/\text{CM.}$

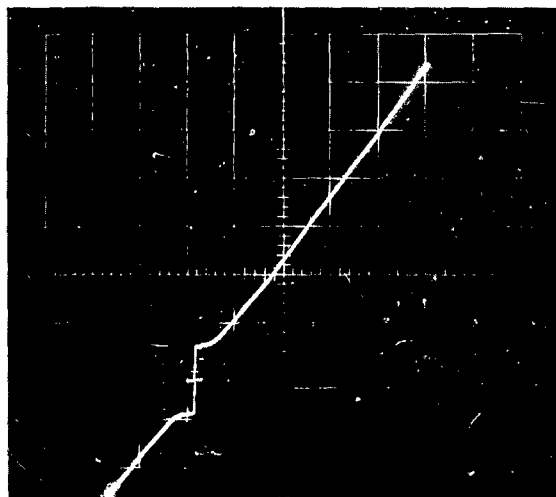


FIGURE 5b I-V CURVE WITH LARGE AC SWEEP SHOWING PERSISTENCE OF JOSEPHSON CURRENT. SCALES: (V) $1.18 \text{ mV}/\text{CM.}$, (H) $133 \mu\text{A}/\text{CM.}$

These criteria are:

1. The zero-voltage currents are sensitive to magnetic fields of only a few gauss. Fine superconducting filaments should show anomalously high, not low critical fields.
2. The currents are always first observed at the lower critical temperature. In view of the laminar superconductor effect, it is unlikely that metallic shorts would always have the same critical temperature as the entire metal film.
3. Calculation of the minimum normal conductance of filaments, based on the current carried at zero-voltage, shows far higher conductance than observed for the single-particle characteristic.
4. The currents cannot be burned out. Despite passing large currents through the junction and developing appreciable voltage across it (several tenths of a volt), the zero-voltage currents remain upon re-examination of the region near the origin. A short should burn out well before this.
5. The ac technique leads to another criterion as shown in Figure 5b. The zero-voltage current is clearly visible in the figure although the ac amplitude is many times the maximum current that can be carried at zero-voltage. Had there been a superconducting short with the indicated critical current, the Joule heat generated when it was normal, i.e., during most of the ac sweep, would have been sufficient to keep it from switching back to the superconducting state during the brief portion of the sweep during which the current amplitude was less than critical.

In closing, it is interesting to note that the Josephson current was most likely present in the first reported observation of the superconducting tunneling phenomenon⁷ in November, 1960. Figure 1 in Reference 7 clearly shows zero-voltage currents similar to those discussed above. In

Reference 7, the authors do not discuss the currents, neither attributing them to shorts nor otherwise referring to them. From the stated sample area and the current magnitude shown in the figure, it is likely, however, that they are indeed Josephson currents.*

III. Millimeter Wave Experiments

Arrangements have been made with Dr. Simon Foner of the National Magnet Laboratory, Massachusetts Institute of Technology, for collaboration on an investigation of tunneltron behavior in high frequency microwave fields. At our laboratory, facilities exist for experimentation at 3 cm. and 1 cm. wavelength. Dr. Foner has facilities for experimentation at 8 mm., 4 mm., and 2 mm., and a 1 mm. facility is planned. The first experiments will employ 4 mm. components fed by either a 4 mm. (70 KMcps) or 2 mm. (140 KMcps) source. The design and construction of the experimental rf head has been completed.

Waveguide, coaxial and dc leads, pumping line, and a micrometer driven tuning rod all pass through vacuum seals on a cover flange. The flange in turn provides a vacuum seal to the top of a small all-metal helium dewar so that the liquid helium may be pumped to achieve temperatures below 4.2° K. A long section of stainless steel waveguide terminates, near the bottom end of the rf head, in a standard 4 mm. waveguide flange. A specially machined section of guide, which serves

*Note: After the closing date of this report (15 April 1963), experiments were carried out on the effect of microwaves on the zero-voltage currents. Several startling effects were observed which will be described fully in the next Interim Engineering Report. A letter describing these effects has been submitted for publication in Physical Review Letters.

as the sample holder, is attached to this flange. A standard 4 mm. shorting plunger, driven by the micrometer controlled tuning rod, rides in a short section of conventional guide which attaches to the sample holder section. This completes the assembly, the bottom portion of which is shown in Figure 6a. The photograph shows a portion of the input stainless steel guide, the sample holder section, the terminating section of guide, and the drive mechanism for the movable shorting plunger. Note that in contrast to the 3 cm. apparatus previously described, no microwave cavity is employed.

The sample holder section of waveguide was machined out of oxygen free copper. It is in two pieces, split lengthwise through the mid-plane of the narrow dimension of the waveguide. One piece, shown in Figure 6b, serves to hold the 2-mil-thick quartz sample substrate, both in the waveguide assembly and in the vacuum evaporator during sample fabrication. The other piece, shown in Figure 7a and enlarged in Figure 7b, provides mechanical support for the contact type electrical leads to the sample. Eight screws fasten the two pieces together to form the waveguide section holding the sample.

The quartz sample substrate, 2 x 24 x 750 mils, rests in a 2-mil-deep groove cut in the copper section transverse to the direction of microwave power flow. (See Figure 6b.) A matching 2-mil-deep groove cut in the other copper piece holds four pressure contacts of 1-mil-thick gold foil, insulated from the copper block by 1-mil-thick Mylar film. (See Figure 7.) When assembled then, the sample sits in the middle of the guide cross-section, a region of maximum microwave electric field in the TE_{10} dominant mode transmission. The shorting plunger enables the standing wave pattern to be shifted relative to the sample.

The two grooves form a channel on each side of the assembled guide that is 4 mils high and 25 mils wide. These channels are beyond cutoff at both 4 mm. and 2 mm. wavelength and should not represent significant power leaks or reflections in the line.

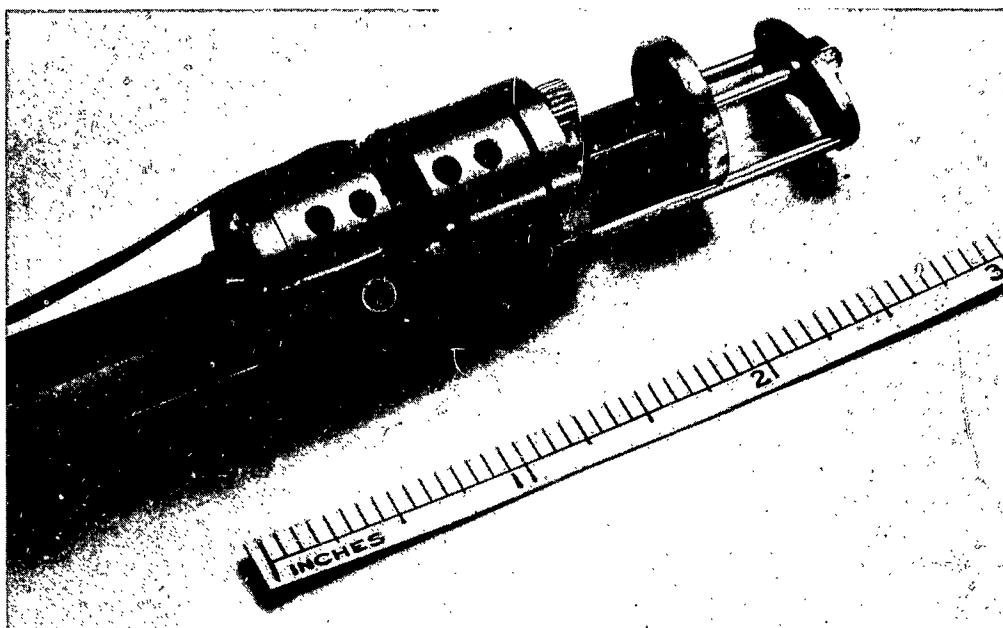


FIGURE 6a BOTTOM SECTION OF ASSEMBLED 4-MM. RF HEAD.

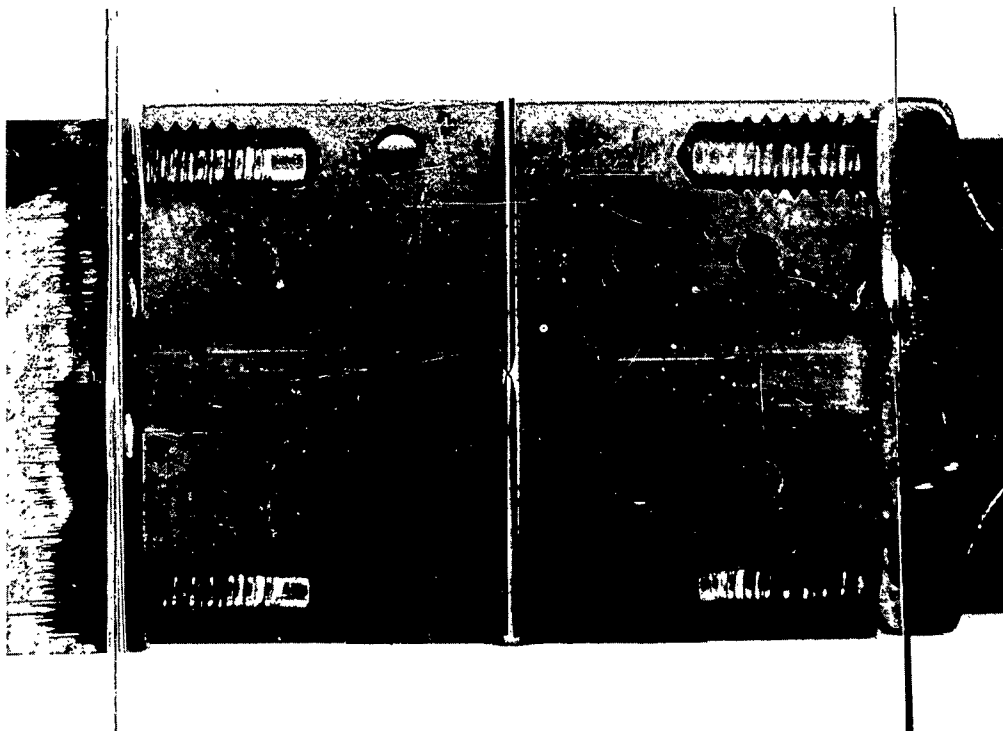


FIGURE 6b ONE HALF OF SPECIAL SECTION SHOWING QUARTZ SUBSTRATE AND SAMPLE IN POSITION.

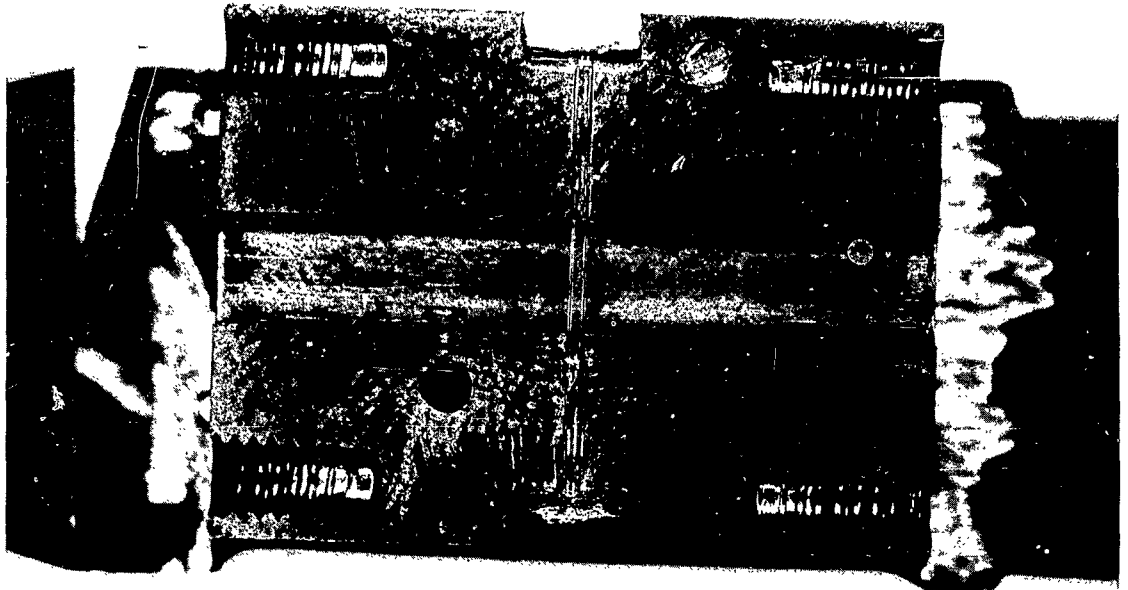


FIGURE 7a OTHER HALF OF SPECIAL SECTION SHOWING MYLAR INSULATING FILM AND GOLD PRESSURE CONTACTS.

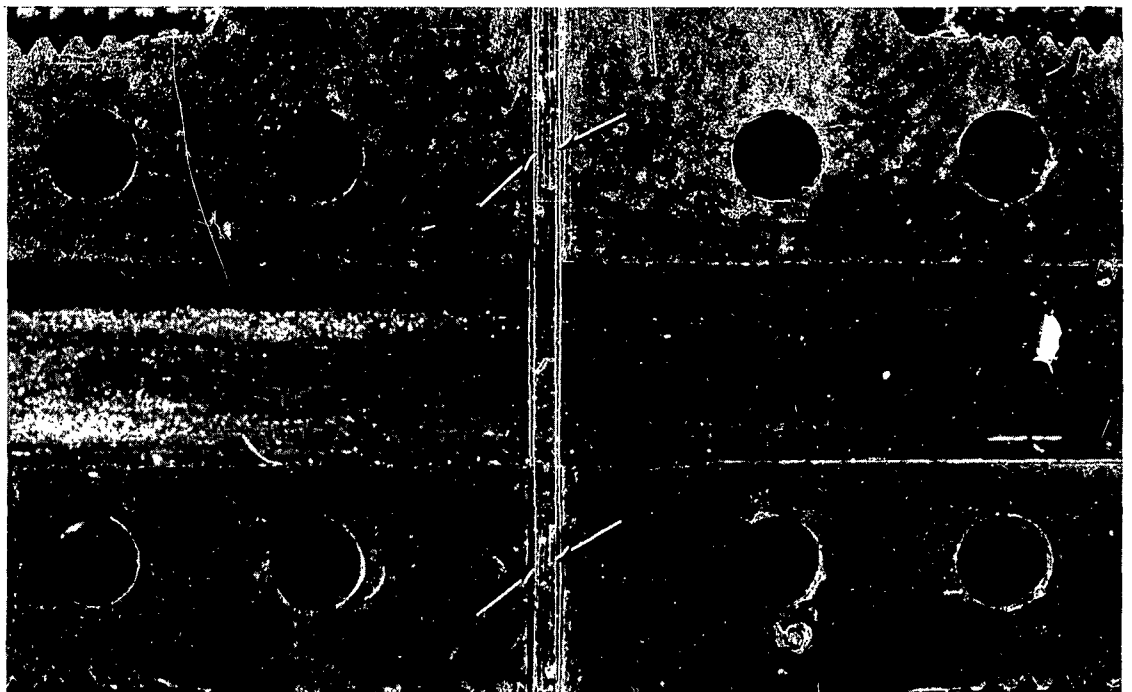


FIGURE 7b ENLARGED VIEW OF ABOVE. GOLD CONTACTS INDICATED BY ARROWS.

One metal film in the sample is in the form of a long 5-mil-wide strip connected by a short diagonal 1-mil-wide strip to another long 5-mil-wide segment. The other film is of the same form but the mirror image of the first so that the 1-mil-wide segments cross and make up a 1-square-mil sample (approx. 6.3×10^{-6} sq. cm.). This simple sample geometry permitted easily fabricated metal masks to be used. The mask slits were formed by spot welding a section of 1-mil brass shim stock to thicker backing material so that a thin edge protrudes. Two coplanar matching pieces, assembled in what constitutes a jig, can be moved relative to one another to form the desired mask slit. Once the jig is assembled to achieve proper registration, all subsequent samples will have that correct registration.

The gold foil contacts the sample over a substantial length of the 5-mil-wide segments but is kept away from the waveguide region. The other ends of the gold contacts are brought around to a terminal plug mounted on the back-side of the copper block. (This side is visible in Figure 6a.)

The design of sample, holder, contacts, etc., was dictated by the desire not to have to handle the fragile substrates and other parts more than the barest minimum. Furthermore, it was clearly impossible to solder to the 5-mil-wide films spaced by only 6 mils from one another and by only 4 mils from the copper block. The result has been that the only delicate step consists in first mounting the quartz substrate. All subsequent steps including sample fabrication follow without delicate handling.

IV. Conclusions

Experiments employing tunneling samples with widely variable resistance and capacitance values and with both thick and thin metal films have failed to reveal any detectable quantum effects in a microwave field. The failure to observe such effects and consequently the discrepancy between our work and that of Dayem and Martin remains unexplained.

The predictions of Josephson that superconducting pairs may indeed tunnel appears to be confirmed by our observations. Josephson's zero-voltage currents have been seen in all samples with adequately thin insulating barriers. They decay toward the familiar single-particle tunneling characteristic by means of negative resistance region. Rf oscillations in this region have been observed in tuned oscillator circuits.

Apparatus has been designed and constructed for extending our experiments to 4 mm. and 2 mm. wavelength. The design goal of ruggedness and ease of handling of the delicate sample has been achieved.

V. Recommendations

It is proposed to study the effect of 3 cm. microwave fields on the Josephson currents. Further, 1 cm. studies on both the Josephson currents and the single-particle tunneling characteristic are to be initiated. Throughout this work, the effect of the pair-tunneling currents on stability, reliability, and reproducibility of tunneling devices for the microwave region needs to be explored.

References

1. Cohen, Falicov, and Phillips, Phys. Rev. Letters 8, 316 (1962).
2. Bardeen, Cooper, and Schrieffer, Phys. Rev. 108, 1175 (1957).
3. B. D. Josephson, Physics Letters 1, 251 (1962).
4. P. W. Anderson and J. M. Rowell, Phys. Rev. Letters 10, 230 (1963).
5. W. Schonbein and P. H. Smith (private communication).
6. V. Ambegaokar and A. Baratoff, Phys. Rev. Letters 10, 486 (1963).
7. Nicol, Shapiro, and Smith, Phys. Rev. Letters 5, 461 (1960).